Desalination and Water Treatment
www.deswater.com

doi: 10.5004/dwt.2018.23045

130 (2018) 124–131
October

Novel green synthesis of a reduced graphene oxide/zinc oxide hybrid nanocomposite adsorbent of *Prunus* × *yedoensis* leaf extract: its catalytic potential to remove phosphate

Velu Manikandan[a], Palanivel Velmurugan[a,b], Sung-Chul Hong[c], Pyong-In Yi[c], Seong-Ho Jang[c], Jeong-Min Suh[c], Eun-Sang Jung[c], Mohammad Russel[d], Subpiramaniyam Sivakumar[c,*]

[a]*Division of Biotechnology, Advanced Institute of Environment and Bioscience, College of Environmental and Bioresource Sciences, Chonbuk National University, Iksan, Jeonbuk 54596, South Korea, emails: mani.env2014@gmail.com (V. Manikandan), palanivelmurugan2008@gmail.com (P. Velmurugan)*
[b]*Department of Microbiology, Sri Sankara Arts and Science College, Enathur, Kanchipuram 631 561, Tamil Nadu, India*
[c]*Department of Bioenvironmental Energy, College of Natural Resource and Life Science, Pusan National University, Miryang-si, Gyeongsangnam-do 50463, Republic of Korea, emails: ssivaphd@yahoo.com (S. Sivakumar), schong@pusan.ac.kr (S.-C. Hong), watec@pusan.ac.kr (P.-I. Yi), jangsh@pusan.ac.kr (S.-H. Jang), suhjm@pusan.ac.kr (J.-M. Suh), esjung@pusan.ac.kr (E.-S. Jung)*
[d]*School of Food and Environment, Dalian University of Technology, Panjin 124221, China, email: mrussel@dlut.edu.cn*

Received 30 November 2017; Accepted 24 August 2018

ABSTRACT

This study describes the synthesis of a reduced graphene oxide/zinc oxide (RGO/ZnO) hybrid nanocomposite using the green process of *Prunus* × *yedoensis* leaf extract and nanocomposites for the removal of phosphate from aqueous solutions. This leaf extract was a reducing agent and was calcined at 500°C for 1 h. The RGO/ZnO nanocomposites' surface morphology and crystal structure were characterized by high-resolution transmission electron microscopy, scanning electron microscopy-energy dispersive spectroscopy, and X-ray powder diffraction. The functional groups were confirmed by Fourier transform infrared spectroscopy and Raman spectroscopy. The surface adsorption characteristics of nanocomposites for the degradation of phosphates were assessed at varying time intervals; phosphate removal via RGO/ZnO nanocomposites was also investigated.

Keywords: Green synthesis; RGO/ZnO nanocomposites; *Prunus* × *yedoensis* leaf extract; Phosphate removal

1. Introduction

The large-scale production of graphene at low cost is of great interest due to its mechanical strength – the two-dimensional carbon layer offers a high surface area and conductivity as well as excellent electron mobility [1]. Because of these characteristics, graphene has been applied to electronics and optoelectronic devices and circuits [2,3]. Graphene oxide (GO) has similar properties to graphene in surface structures including a series of reactive oxygen functional groups on the sheet surface with chemical and carboxyl groups (carboxylic acid, hydroxyl, and epoxide). These similarities enable the preparation of reduced graphene oxide (RGO) containing nanocomposites [2,3].

The chemical conversion of graphite is typically obtained via oxidation of graphite oxide powder via the modified Hummer and Staudenmeier methods [4,5]. The green syntheses of graphene oxide [6–10] and zinc oxide nanoparticles [11–16] use various natural materials. Several chemical reducing agents can reduce graphene oxide sheets:

* Corresponding author.

hydrazine [17–19], sodium borohydrate [20,21], hydroquinone [22], gaseous hydrogen [23], and alkaline solutions [24]. Thermal treatment also reduces graphene oxide when it removes functional groups such as oxides from the surface [25,26]. Currently, nanosized materials can be fabricated using green eco-friendly methods. The extracts are prepared from plants or fruits and used as stabilizers and capping agents to control crystal growth [27]. Previously, graphene nanosheets were successfully synthesized from GO with pomegranate juice [28]. Here, *Prunus* × *yedoensis* leaf extracts were used for the fabrication of RGO/ZnO nanocomposites.

Prunus × *yedoensis* leaf extracts are cost effective because they are very common in South Korea. Plant leaf extracts play a vital role as reducing and capping agents in the synthesis of nanocomposites. Previously, Velmurugan et al. [29,30] used *Prunus* × *yedoensis* leaf extracts to produce silver and zinc oxide nanoparticles and examine their antibacterial activity. Here, for the first time, *Prunus* × *yedoensis* leaf extract was used as a reducing agent for synthesized graphene oxide/zinc oxide (RGO/ZnO) nanocomposites and then deployed this material to remove phosphate from aqueous solutions.

2. Materials and methods

2.1. Chemicals

Graphite powder (Sigma, Kawasaki, Japan), $KMnO_4$ (>99%, Sigma), $NaNO_3$ (>99%, Sigma), H_2SO_4 (reagent grade), H_2O_2 (30%, VWR Chemicals, South Korea), $Zn(NO_3)_2$ (>98%, Sigma), Na_2HPO_4 (>99%, Sigma), and methanol (DaeJung Chemicals Reagent Co. Ltd., South Korea) were used without purification. Milli-Q water (18 μΩ/m conductivity and <3 ppb total organic carbon; Barnstead, Waltham, MA, USA) was used as the solvent.

2.2. Prunus × yedoensis leaf extract

The matured leaves of *Prunus* × *yedoensis* were collected from Miryang City, South Korea. The leaves (100 g) were washed with distilled water and cut into small pieces. The leaves were then boiled in 250 mL of sterile nanopure water for 30 min; this was done in a heating mantle with a round bottom flask to capture the extract. The leaf extract was filtered with Whatman No. 42 filter paper; the extract was collected in a 250-mL Erlenmeyer flask and stored at 4°C until further use.

2.3. Synthesis of GO

GO was fabricated as described by the modified Hummer's method through oxidation and exfoliation of commercially available graphite [28,31,32]. Graphite flake (1 or 2 g) and sodium nitrate were mixed in an Erlenmeyer flask kept in an ice bath. 96 mL of concentrated H_2SO_4 was gradually added to the reaction mixture with vigorous stirring at 0°C–15°C for 1 h. Next, 6 g of $KMnO_4$ was slowly added (20°C must be maintained) and stirred it again for 1 h. The reaction mixture temperature was then raised to 35°C and stirred for 2 h. Then, 150 mL of 70°C distilled water was added and stirred for 15 min followed by 10 mL H_2O_2 and 55 mL of water to reduce the residual permanganate to soluble manganese ions. The resulting suspension was filtered and washed by centrifugation with 5% HCl (2,500 rpm, 10 min, four times) and then water (2,500 rpm, 10 min, four times); the product was finally dried at 60°C for 24 h to obtain graphite oxide powder.

2.4. Reduction of graphene oxide

To prepare RGO, an approximate volume of 500 mL of *Prunus* × *yedoensis* leaf extract (PYLE) was taken to mix with the GO dispersion (1 g) with stirring for 24 h at 80°C using a magnetic stirrer. Next, the dispersed solution was sonicated for 30 min and centrifuged at 12,000 rpm. It was then washed several times with nanopure water and dried at 100°C for 24 h [33].

2.5. Synthesis of RGO/ZnO nanocomposites

The resulting RGO powder (0.5 g) was prepared with a green method using aqueous PYLE extract added to 300 mL; the reaction mixture was constantly stirred for 1 h. The mixture was ultra-sonicated for 1 h and then treated with 100 mL of 0.1 M $Zn(NO_3)_2$ using a peristaltic pump (0.5 mL/h) at 80°C with a magnetic stirrer. Later, the RGO/ZnO-Ellagate complex was centrifuged at 12,000 rpm and washed several times with methanol:water (1:1) several times to remove organic residues. The resulting product was calcined at 500°C for 1 h to produce a fine powder that was carefully characterized and investigated for catalysis.

2.6. Characterization of RGO/ZnO nanocomposites

The RGO/ZnO nanocomposites were characterized using high-resolution transmission electron microscopy (HR-TEM model, JEOL-2010, Akishima, Tokyo, Japan); selected area electron diffraction (SAED) patterns assessed the surface morphology, size, and crystalline structure of the RGO/ZnO nanocomposite. PYLE-fabricated RGO/ZnO nanocomposite surface structures including their texture and elements were examined with a scanning electron microscopy-energy dispersive spectroscopy (SEM-EDS; JSM-6400 JEOL; Japan Electron Optics Ltd., Tokyo, Japan). X-ray powder diffraction of the nanocomposite was obtained with an X-ray diffraction system (Rigaku X-ray Diffractometer, Tokyo, Japan) working from the 2θ-range of 20°–80° with a step size of 0.02°. A Fourier transform infrared spectroscope (Perkin-Elmer FTIR spectrophotometer, Norwalk, CT, USA) was used to study the phytoconstituents and RGO/ZnO nanocomposites from 4,000 to 400 cm^{-1} to analyze the nanocomposites' functional groups in diffuse reflectance mode at a resolution of four particles per centimeter in KBr pellets. Raman spectra were recorded using the Xplora spectrometer from Horiba Scientific (Edison, NJ, USA) with a wavelength of 532 nm. The RGO/ZnO nanocomposites were obtained from PYLE at ambient temperature and were used to remove phosphate. The UV-visible (UV-Vis) absorption measurements were taken with a UV-Vis spectrum diode-array spectrophotometer (UV-1800, Shimadzu, Kyoto, Japan) from 300 to 800 nm using a glass cuvette with a cm^{-1} optical path.

2.7. Photocatalytic activity

The catalytic activity of the RGO/ZnO nanocomposite adsorbent was estimated by measuring the photodegradation

of phosphate aqueous solution under sunlight radiation with a UV-Vis spectrophotometer [34]. All reactions were carried out at a natural pH at room temperature (25°C). The reaction suspensions were prepared by adding 10 mg of RGO/ZnO nanocomposite catalyst in 100 mL of aqueous phosphate solution at an initial concentration of 10 ppm/L; these were added to the vessels and the solution mixture and kept in the sunlight for photodegradation. After a defined irradiation time, the suspension was monitored for color removal at 5-min intervals (0, 5, 10, 15, 20, 25, 30, 35, 40, 45, 50, 55, and 60 min). All experiments occurred between 11:00 am and 2:00 pm under direct sunlight radiation. The phosphate aqueous solution was removed, centrifuged, and filtered to estimate the available concentration using a UV-Vis spectrophotometer at 690 nm [35]. The percentage of phosphate degradation was calculated via the following formula:

$$\text{Percentage of degradation} = \frac{C_0 - C_t}{C_0} \times 100$$

where C_0 is the initial concentration of phosphate aqueous solutions (mg/L) and C_t is the concentration of aqueous solutions at selected time intervals from irradiation (mg/L).

3. Results and discussion

3.1. Fabrication and characterization of RGO/ZnO nanocomposite

This study is an eco-friendly approach to the green synthesis of RGO/ZnO nanocomposites using *Prunus* × *yedoensis* leaf extract. Fig. 1(a) diagrams the experimental procedure. Graphite powder was first modified with Hummer's method [20], that is, graphite was oxidized into GO by exfoliation. The GO was then reduced into RGO under mild conditions using PYLE as a natural reducing agent [28]. It was prepared by directly boiling the matured leaves of *Prunus* × *yedoensis* with nanopure water [36]. The RGO was then slowly added to the PYLE and sonicated for 30 min to get a *homogenous suspension* of RGO followed by a mixture of $Zn(NO_3)_2$ with a peristaltic pump. The solution was centrifuged and washed five times with methanol and nanopure water to remove organic residues. This purified composite product was transferred to a ceramic crucible for calcination at 500°C for 2 h to merge with the RGO/ZnO nanocomposite. Our results coincide with previous reports on the fabrication of RGO/ZnO nanocomposites with pomegranate juice [28], carrot root aqueous extract [37], and clove extract [33].

Figs. 2(a)–(d) show HR-TEM images and the SAED pattern of RGO/ZnO nanocomposites prepared with a green material and calcination. Fig. 2 shows the HR-TEM images of RGO/ZnO adsorbents at various magnifications (Figs. 2(a) 100 nm; 2(b) 50 nm; 2(c) 20 nm). This demonstrates its high surface area that actively and readily adsorbs phosphate molecules. The SAED pattern shows that the particles have a narrow size distribution with good crystallinity in the RGO nanosheet on Zn nanoparticles (Fig. 2(d)).

The EDS spectra (Fig. 3(c)) confirmed the preparation and purity of RGO/ZnO nanocomposites via the absence of peaks other than RGO/ZnO peaks. The SEM-EDS images of Zn nanoparticles illustrate that Zn and O predominated; the C peak indicates coating of the RGO sample. Figs. 3(a) and (b) represent SEM micrographs of RGO/ZnO nanocomposites via different morphological structures and sizes including the elemental composition of Zn and O [32].

The XRD pattern (Fig. 4(a)) shows that the synthesis of the RGO/ZnO nanocomposite depends on the production method and calcination temperature. The diffraction peaks at 2θ values of 25.0° and 43.0° correspond to the (101) and (110) planes, respectively [38,39]. The peaks show the formation of the crystal phase of the RGO/ZnO nanocomposite; the functional groups in the green PYLE-mediated and reduced RGO/ZnO nanocomposite were determined via Fourier

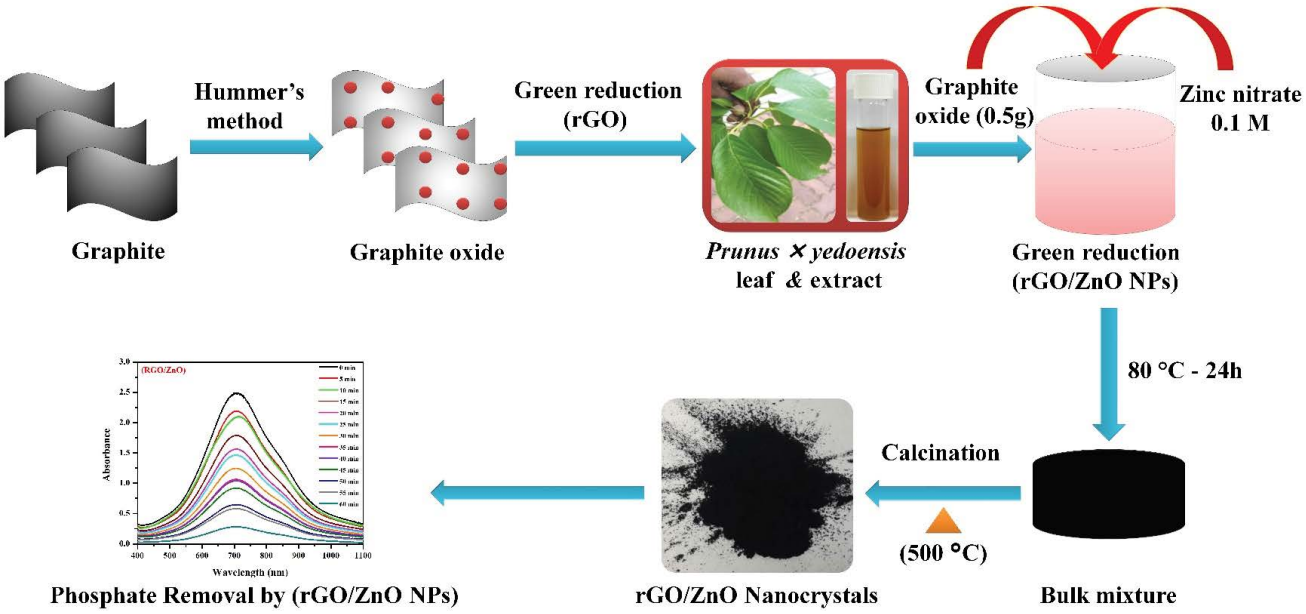

Fig. 1. RGO/ZnO nanocomposite synthesis and their utility in photodegradation.

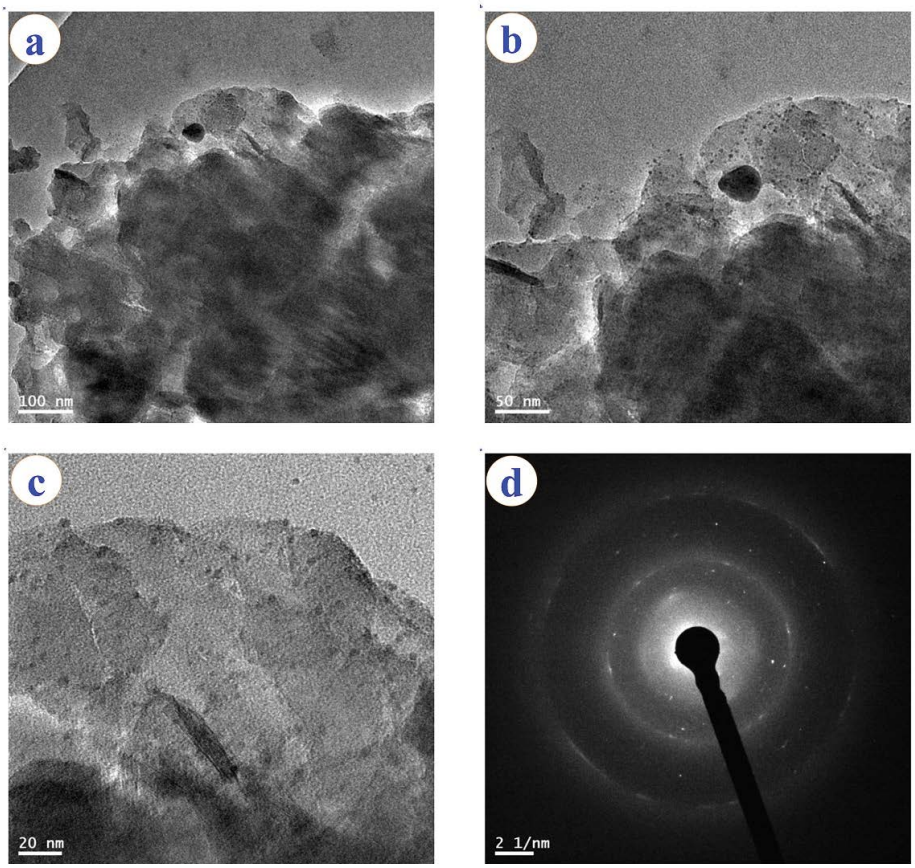

Fig. 2. HR-TEM images at different magnifications: (a) 100 nm, (b) 50 nm, (c) 20 nm, and (d) SAED patterns.

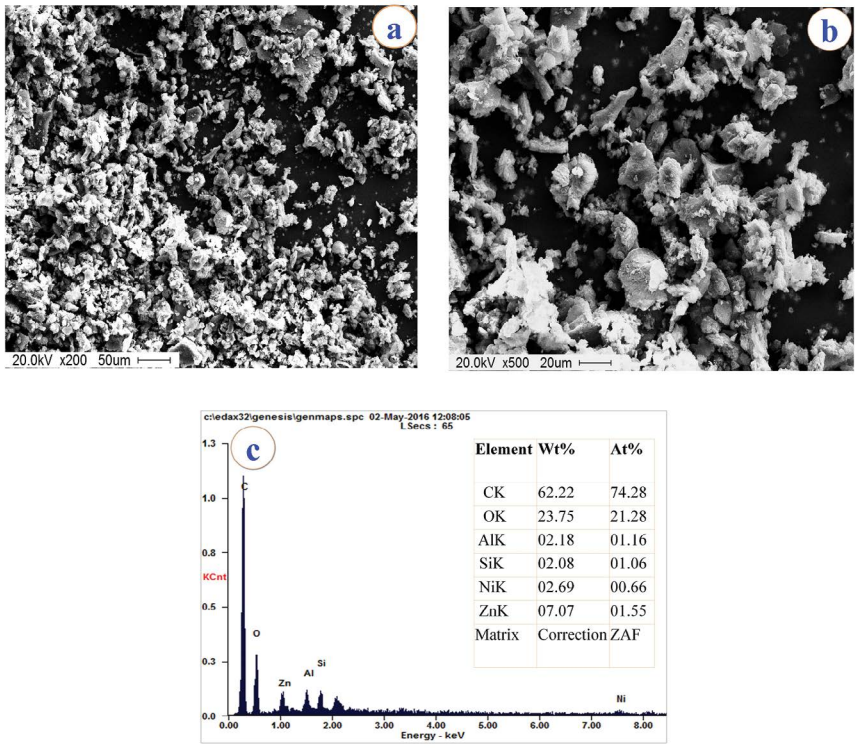

Fig. 3. Characterization of RGO/ZnO nanocomposites: (a) and (b) SEM images; (c) EDS.

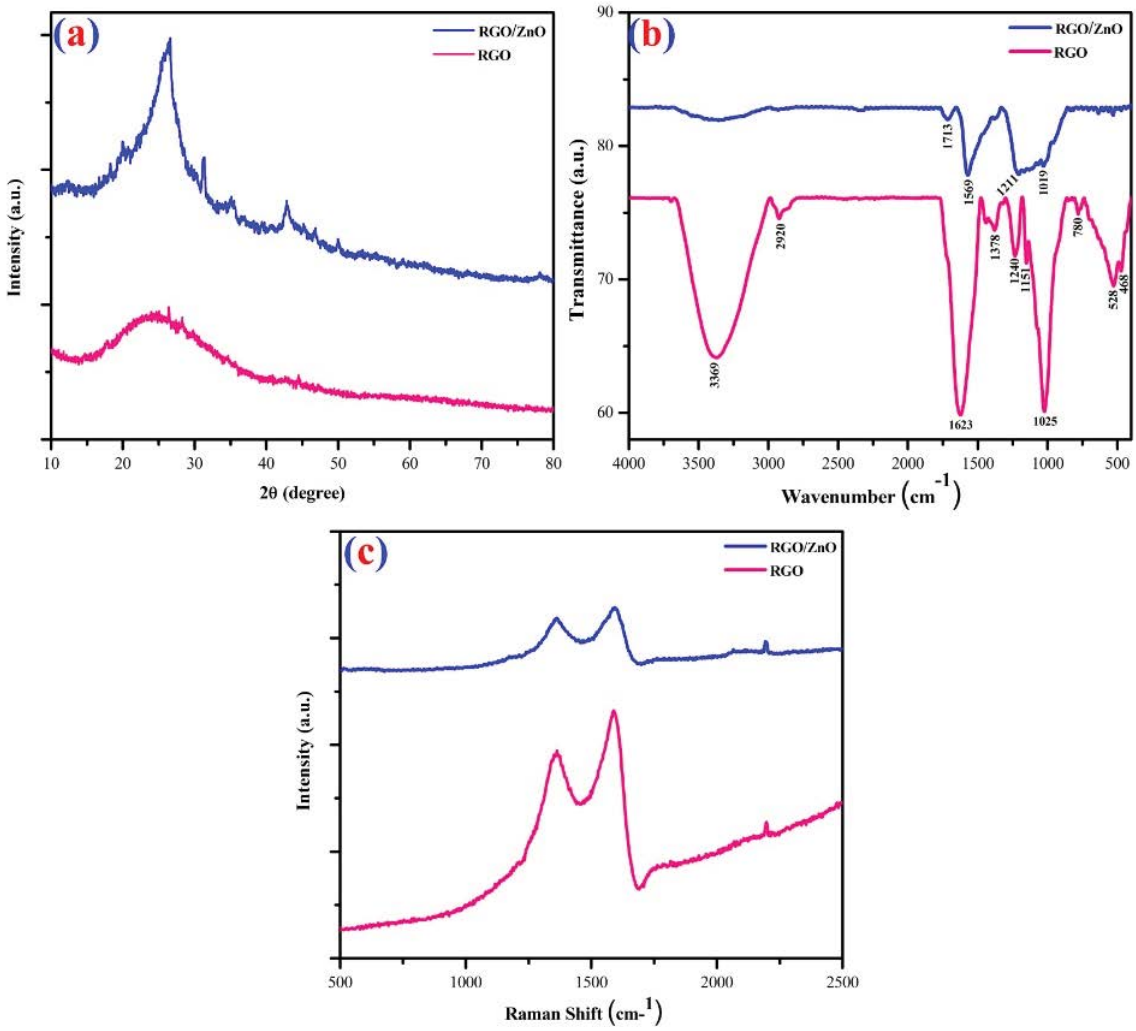

Fig. 4. Characterization of RGO/ZnO nanocomposites: (a) XRD, (b) FTIR, and (c) Raman spectra.

transform infrared spectroscopy (Fig. 4(b)). The RGO characteristic bands at 3,369, 2,920, 1,623, 1,378, 1,240, 1,151, 1,025, 780, 528, and 468 cm^{-1} became RGO/ZnO nanocomposite bands at 1,713, 1,569, 1,211, 3,369, and 1,019 cm^{-1}. These are attributed to N–H, C–H, C=O, and C–OH stretching vibrations, respectively [30]. Fig. 4(c) shows Raman spectroscopy results of pure RGO and RGO/ZnO nanocomposites as well as characteristic peaks centered at 1,300 cm^{-1} (D, the breathing mode of k-point photons of A_1g symmetry) and 1,620 cm^{-1} (G, E_{2g} phonon of sp2 carbon atoms), respectively [32,39].

3.2. Photocatalytic experiments of RGO/ZnO nanocomposite

The catalytic activity of RGO/ZnO nanocomposite adsorbent was examined via the removal of phosphate as a key pollutant. Fig. 5 shows the removal capacity of the RGO/ZnO nanocomposite via the efficient adsorption of the green-fabricated samples. Our results confirm that this is the most efficient treatment time for the removal of phosphate via PYLE synthesis of RGO/ZnO nanocomposites (10 mg/50 mL/10 ppm) (Fig. 5(a)). The adsorption study was standardized for phosphate removal in the first 5 min. It gradually increased to equilibrium at 60 min; this required less contact time to reach equilibrium and showed a higher adsorption rate.

The RGO/ZnO nanocomposite was prepared via green chemistry (plant extracts and calcination). The phosphate concentration (C_t/C_0) versus time under sunlight irradiation was plotted for RGO, ZnO, and RGO/ZnO photocatalysts. Here, C_t is the concentration after different times and C_0 is the original concentration of phosphate (Fig. 5(b)). These results show that the RGO/ZnO composite has more degradation efficiency than RGO and ZnO. The phosphate absorption decreased after degradation using the RGO/ZnO nanocomposite catalyst. Concurrently, the gradual color change suggests that the phosphate molecules underwent oxidation (Fig. 5(c)). The adsorption study was standardized for phosphate removal using an initial time period of 5 min – this gradually increased to an equilibrium time of 60 min. The RGO/ZnO nanocomposite required less contact time to reach equilibrium, and it showed a higher adsorption rate.

One issue for phosphate ion degradation is selectivity. There is likely competition between phosphate ions and other coexisting anions. The RGO can absorb more phosphate

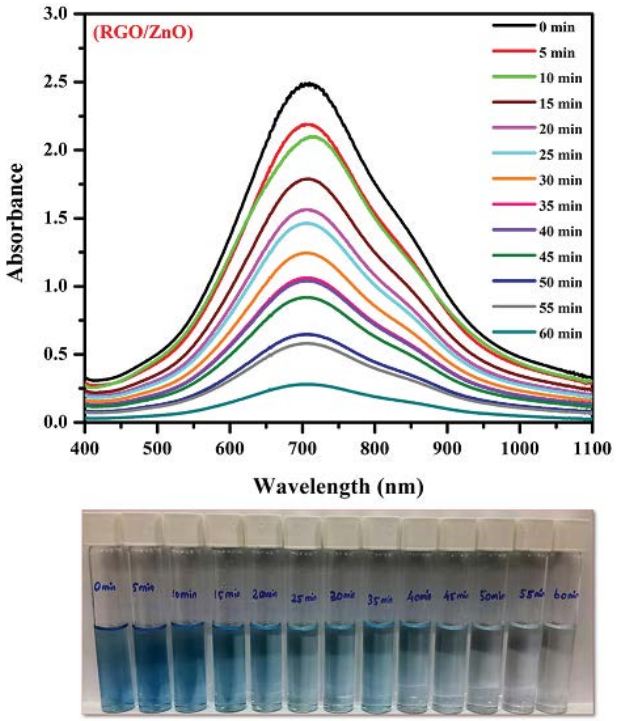

Fig. 5. UV-Vis absorption spectra of aqueous phosphate solution in the presence of RGO/ZnO nanocomposites at different time intervals.

molecules on its surface, and the introduction of RGO enlarges the light adsorption scope to enhance the efficiency of simulated sunlight. Due to its 2D π-conjugation structure, RGO can act as a photo-electron acceptor allowing the excited electrons of ZnO in the composites to be rapidly transferred from the transmission band of ZnO to the RGO.

3.3. Mechanism of phosphate degradation by RGO/ZnO nanocomposites

The proposed mechanisms behind the photocatalytic efficiency of the green synthesized RGO-ZnO composites and ZnO or RGO particles alone for the photodegradation of phosphate are described below. Phosphate solutions under irradiation without any photocatalysts serve as the blank. The RGO–ZnO composites show the most superior photocatalytic performance among RGO–ZnO nanocrystals – this might be due to their crystallinity and synergistic effects with RGO. The enriched photocatalytic activity of RGO/ZnO nanocomposites was attributed to the more effective separation of e^-/h^+ pairs [40]. This occurs due to high crystallinity of the composite, which enhances the generation of electron–hole pairs and reduces the number of defects to prevent electron–hole pairs from recombining. However, the improvements in crystallinity are often accompanied by increasing particle sizes and stacks of layered RGO. This is not conductive to the formation of many active sites. The initial photo-excitation occurs in an adsorbate molecule that then interacts with the

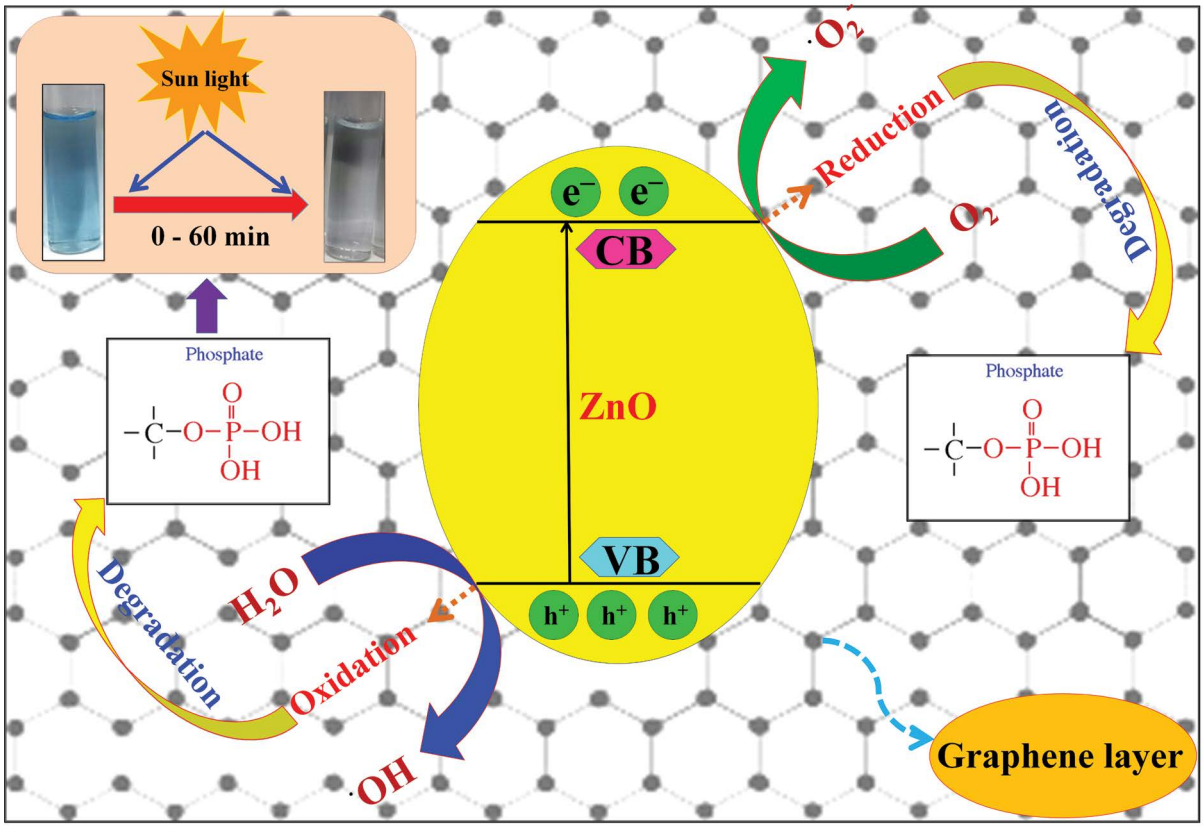

Fig. 6. Photocatalytic mechanism of RGO/ZnO nanocomposites for the degradation of phosphate.

ground state catalyst substrate. In a catalyzed photoreaction, an electronic transmission is forbidden by the separation between the molecule and the catalyst substrate [41].

The enriched photocatalytic activity of RGO/ZnO nanocomposites was attributed to the more effective separation of e^-/h^+ pairs [40]. This occurs for wavelengths of light that are equal to or greater than the bandgap of RGO/ZnO. Previously, Atchudan et al. [40] reported that the electrons receive energy and transfer electrons from the valence band (VB) to the conduction band (CB). This forms a hole (h^+) in the VB and an electron (e^-) in the CB. The photo-excited hole (h^+) can lead to direct oxidative degradation of adsorbed phosphate, or these excitons can oxidize adsorbed molecules to form a reactive $^{\bullet}OH$ radical that oxidizes organic pollutants. The photogenerated electrons react with the absorbed O_2 on the edge of carbon textiles to produce $OH^{\bullet}$ [42]. These hydroxyl radicals are very reactive oxidative species that react with the organic or water pollutants and can be degraded to CO_2 and H_2O. In addition, the remaining holes in the VB of RGO/ZnO nanocomposites can take part in the redox reaction to generate $OH^{\bullet}$, which is further used to remove phosphate under sunlight irradiation. The degradation pathway of phosphate can be given via the following equations (Eqs. (1)–(5)):

$$\mathrm{RGO/ZnO} + h\upsilon \rightarrow \mathrm{RGO/ZnO}\left(h_{VB}^{+}\right) + \mathrm{RGO/ZnO}\left(e_{CB}^{-}\right) \quad (1)$$

Here, RGO/ZnO $\left(h_{VB}^{+}\right)$ is the positive hole in the VB, and RGO/ZnO $\left(e_{CB}^{-}\right)$ is the photo-excited electron in the CB.

$$\mathrm{RGO/ZnO}\left(h_{VB}^{+}\right) + H_2O_{ads} \rightarrow \mathrm{RGO/ZnO} + {}^{\bullet}OH + H^{+} \quad (2)$$

$$^{\bullet}OH + \text{Phosphate ions} \rightarrow CO_2 + H_2O \quad (3)$$

$$\mathrm{RGO/ZnO}\left(e_{CB}^{-}\right) + O_{2ads} \rightarrow \mathrm{RGO/Zno} + O_{2ads}^{\bullet -} \quad (4)$$

$$O_2^{-\bullet} + \text{Phosphate ions} \rightarrow CO_2 + H_2O \quad (5)$$

The efficient adsorption of target pollutants to RGO/ZnO results in complete photodegradation under sunlight. A proposed photocatalytic reaction mechanism is represented in the schematic diagram shown in Fig. 6.

4. Conclusion

This study used RGO/ZnO nanocomposites from the green reduction of *Prunus* × *yedoensis* leaf extract for removal of aqueous phosphate. The presence of phytochemicals in the leaf extract helps in the synthesis of metal oxide nanoparticles by inducing oxidation and reduction. The amines and alkanes on the phytochemicals induce nanoparticle synthesis and are common in secondary metabolites such as terpenoids, flavonoids, and alkaloids. The nanocomposites are efficient at removing phosphates from aqueous solutions. This study illustrates the efficiency of this common plant for waste remediation.

References

[1] Q. Xiang, J. Yu, M. Jaroniec, Graphene-based semiconductor photocatalysts, Chem. Soc. Rev., 41 (2012) 782–796.
[2] X. Wang, L. Zhi, K. Müllen, Transparent, conductive graphene electrodes for dye-sensitized solar cells, Nano Lett., 8 (2008) 323–327.
[3] P. Blake, P.D. Brimicombe, R.R. Nair, T.J. Booth, D. Jiang, F. Schedin, L.A. Ponomarenko, S.V. Morozov, H.F. Gleeson, E.W. Hill, A.K. Geim, K.S. Novoselov, Graphene-based liquid crystal device, Nano Lett., 8 (2008) 1704–1708.
[4] W.S. Hummers Jr., R.E. Offeman, Preparation of graphitic oxide, J. Am. Chem. Soc., 80 (1958) 1339.
[5] L. Staudenmaier, Verfahren zur darstellung der graphitsaure, Eur. J. Inorg. Chem., 31 (1898) 1481–1487.
[6] D. Zhang, X. Liu, X. Wang, Green synthesis of graphene oxide sheets decorated by silver nanoprisms and their anti-bacterial properties, J. Inorg. Biochem., 105 (2011) 1181–1186.
[7] L. Wu, P. Qu, P.R. Zhou, B. Wang, S. Liao, Green synthesis of reduced graphene oxide and its reinforcing effect on natural rubber composites, High Perform. Polym., 27 (2015) 486–496.
[8] C. Rodríguez-González, P. Velázquez-Villalba, P. Salas, V.M. Castaño, Green synthesis of nanosilver-decorated graphene oxide sheets, IET Nanobiotechnol., 10 (2016) 301–307.
[9] W.K. Park, Y. Yoon, S. Kim, S.Y. Choi, S. Yoo, Y. Do, S. Jung, D.H. Yoon, H. Park, W.S. Yang, Toward green synthesis of graphene oxide using recycled sulfuric acid via Couette–Taylor flow, ACS Omega, 2 (2017) 186–192.
[10] S. Pei, Q. Wei, K. Huang, H.M. Cheng, W. Ren, Green synthesis of graphene oxide by seconds timescale water electrolytic oxidation, Nat. Commun., 9 (2018) 145.
[11] H. Agarwal, S. Venkat Kumar, S. Rajeshkumar, A review on green synthesis of zinc oxide nanoparticles – an eco-friendly approach, Resour.-Effic. Technol., 3 (2017) 406–413.
[12] J. Santhoshkumar, S.V. Kumar, S. Rajeshkumar, Synthesis of zinc oxide nanoparticles using plant leaf extract against urinary tract infection pathogen, Resour.-Effic. Technol., 3 (2017) 459.
[13] A.C. Dhanemozhi, V. Rajeswari, S. Sathyajothi, Green synthesis of zinc oxide nanoparticle using green tea leaf extract for super capacitor application, Mater. Today: Proc., 4 (2017) 660–667.
[14] S.K. Chaudhuri, L. Malodia, Biosynthesis of zinc oxide nanoparticles using leaf extract of *Calotropis gigantea*: characterization and its evaluation on tree seedling growth in nursery stage, Appl. Nanosci., 7 (2017) 501–512.
[15] N. Bala, S. Saha, M. Chakraborty, M. Maiti, S. Das, R. Basu, P. Nandy, Green synthesis of zinc oxide nanoparticles using *Hibiscus subdariffa* leaf extract: effect of temperature on synthesis, anti-bacterial activity and anti-diabetic activity, RSC Adv., 5 (2015) 4993–5003.
[16] P. Sutradhar, M. Saha, Green synthesis of zinc oxide nanoparticles using tomato (*Lycopersicon esculentum*) extract and its photovoltaic application, J. Exp. Nanosci., 11 (2016) 314–327.
[17] G. Eda, G. Fanchini, M. Chhowalla, Large-area ultrathin films of reduced graphene oxide as a transparent and flexible electronic material, Nat. Nanotechnol., 3 (2008) 270–274.
[18] C. Gómez-Navarro, R.T. Weitz, A.M. Bittner, M. Scolari, A. Mews, M. Burghard, K. Kern, Electronic transport properties of individual chemically reduced graphene oxide sheets, Nano Lett., 7 (2007) 3499–3503.
[19] C.G. Lee, S. Park, R.S. Ruoff, A. Dodabalapur, Integration of reduced graphene oxide into organic field-effect transistors as conducting electrodes and as a metal modification layer, Appl. Phys. Lett., 95 (2009) 1–3.
[20] A.B. Bourlinos, D. Gournis, D. Petridis, T. Szabó, A. Szeri, I. Dékány, S. Tudomanyegyetem, Graphite oxide: chemical reduction to graphite and surface modification with primary aliphatic amines and amino acids, Langmuir, 19 (2003) 6050–6055.
[21] H.J. Shin, K.K. Kim, A. Benayad, S.M. Yoon, H.K. Park, I.S. Jung, M.H. Jin, H.K. Jeong, J.M. Kim, J.Y. Choi, Y.H. Lee, Efficient reduction of graphite oxide by sodium borohydride and its effect on electrical conductance, Adv. Funct. Mater., 19 (2009) 1987–1992.
[22] S. Wang, P.J. Chia, L.L. Chua, L.H. Zhao, R.Q. Png, S. Sivaramakrishnan, M. Zhou, R.G.S. Goh, R.H. Friend, A.T.S. Wee, P.K.H. Ho, Band-like transport in surface-functionalized highly solution-processable graphene nanosheets, Adv. Mater., 20 (2008) 3440–3446.

[23] Z.S. Wu, W. Ren, L. Gao, B. Liu, C. Jiang, H.M. Cheng, Synthesis of high-quality graphene with a pre-determined number of layers, Carbon, 47 (2009) 493–499.
[24] X. Fan, W. Peng, Y. Li, X. Li, S. Wang, G. Zhang, F. Zhang, Deoxygenation of exfoliated graphite oxide under alkaline conditions: a green route to graphene preparation, Adv. Mater., 20 (2008) 4490–4493.
[25] H.C. Schniepp, J.L. Li, M.J. McAllister, H. Sai, M. Herrera-Alonso, D.H. Adamson, R.K. Prud'homme, R. Car, D.A. Saville, I.A. Aksay, Functionalized single graphene sheets derived from splitting graphite oxide, J. Phys. Chem. B, 110 (2006) 8535–8539.
[26] S. Stankovich, D.A. Dikin, G.H.B. Dommett, K.M. Kohlhaas, E.J. Zimney, E.A. Stach, R.D. Piner, S.T. Nguyen, R.S. Ruoff, Graphene-based composite materials, Nature, 442 (2006) 282–286.
[27] F. Tavakoli, M. Salavati-Niasari, F. Mohandes, Green synthesis of flower-like CuI microstructures composed of trigonal nanostructures using pomegranate juice, Mater. Lett., 100 (2013) 133–136.
[28] F. Tavakoli, M. Salavati-Niasari, F. Mohandes, Green synthesis and characterization of graphene nanosheets, Mater. Res. Bull., 63 (2015) 51–57.
[29] P. Velmurugan, M. Cho, S.S. Lim, S.K. Seo, H. Myung, K.S. Bang, S. Sivakumar, K.M. Cho, B.T. Oh, Phytosynthesis of silver nanoparticles by *Prunus yedoensis* leaf extract and their antimicrobial activity, Mater. Lett., 138 (2015) 272–275.
[30] P. Velmurugan, J. Shim, K. Kim, B.T. Oh, *Prunus* × *yedoensis* tree gum mediated synthesis of platinum nanoparticles with antifungal activity against phytopathogens, Mater. Lett., 174 (2016) 61–65.
[31] Y. Wang, J. Liu, L. Liu, D.D. Sun, High-quality reduced graphene oxide-nanocrystalline platinum hybrid materials prepared by simultaneous co-reduction of graphene oxide and chloroplatinic acid., Nanoscale Res. Lett., 6 (2011) 241.
[32] H. Moussa, E. Girot, K. Mozet, H. Alem, G. Medjahdi, R. Schneider, ZnO rods/reduced graphene oxide composites prepared via a solvothermal reaction for efficient sunlight-driven photocatalysis, Appl. Catal., B, 185 (2016) 11–21.
[33] D. Suresh, H. Nagabhushana, S.C. Sharma, Clove extract mediated facile green reduction of graphene oxide, its dye elimination and antioxidant properties, Mater. Lett., 142 (2015) 4–6.
[34] APHA, Standard Methods for the Examination of Water and Wastewater, American Public Health Association, 21th ed., APHA-AWWA-WEF, Washington, DC, USA, 2001.
[35] S. Ragupathy, K. Raghu, P. Prabu, Synthesis and characterization of TiO_2 loaded cashew nut shell activated carbon and photocatalytic activity on BG and MB dyes under sunlight radiation, Spectrochim. Acta, Part A, 138 (2015) 314–320.
[36] V. Manikandan, P. Velmurugan, J.H. Park, N. Lovanh, S.K. Seo, P. Jayanthi, Y.J. Park, M. Cho, B.T. Oh, Synthesis and antimicrobial activity of palladium nanoparticles from *Prunus* × *yedoensis* leaf extract, Mater. Lett., 185 (2016) 335–338.
[37] T. Kuila, S. Bose, P. Khanra, A.K. Mishra, N.H. Kim, J.H. Lee, A green approach for the reduction of graphene oxide by wild carrot root, Carbon, 50 (2012) 914–921.
[38] J. Qin, X. Zhang, C. Yang, M. Cao, M. Ma, R. Liu, ZnO microspheres-reduced graphene oxide nanocomposite for photocatalytic degradation of methylene blue dye, Appl. Surf. Sci., 392 (2017) 196–203.
[39] M. Vinothkannan, C. Karthikeyan, G. Gnana kumar, A.R. Kim, D.J. Yoo, One-pot green synthesis of reduced graphene oxide (RGO)/Fe_3O_4 nanocomposites and its catalytic activity toward methylene blue dye degradation, Spectrochim. Acta, Part A, 136 (2015) 256–264.
[40] R. Atchudan, T.N.J.I. Edison, S. Perumal, D. Karthikeyan, Y.R. Lee, Facile synthesis of zinc oxide nanoparticles decorated graphene oxide composite via simple solvothermal route and their photocatalytic activity on methylene blue degradation, J. Photochem. Photobiol., B, 162 (2016) 500–510.
[41] J. He, C. Niu, C. Yang, J. Wang, X. Su, Reduced graphene oxide anchored with zinc oxide nanoparticles with enhanced photocatalytic activity and gas sensing properties, RSC Adv., 4 (2014) 60253–60259.
[42] N.P. Herring, S.H. Almahoudi, C.R. Olson, M.S. El-Shall, Enhanced photocatalytic activity of ZnO–graphene nanocomposites prepared by microwave synthesis, J. Nanopart. Res., 14 (2012) 1277.